Optical properties of the interband transitions of layered gallium sulfide

C. H. Ho and S. L. Lin

Citation: Journal of Applied Physics **100**, 083508 (2006); doi: 10.1063/1.2358192
View online: http://dx.doi.org/10.1063/1.2358192
View Table of Contents: http://aip.scitation.org/toc/jap/100/8
Published by the American Institute of Physics

Optical properties of the interband transitions of layered gallium sulfide

C. H. Ho[a] and S. L. Lin
Department of Materials Science and Engineering, National Dong Hwa University, Shoufeng, Hualien 97401, Taiwan, Republic of China

(Received 18 April 2005; accepted 23 August 2006; published online 20 October 2006)

Optical properties of GaS layered semiconductor have been characterized using temperature-dependent absorption and piezoreflectance (PzR) measurements in the temperature range between 15 and 300 K. From the comparison of optical-absorption and PzR spectra at low temperature, the gallium sulfide layer was confirmed to be an indirect semiconductor. The band gap of GaS was determined to be 2.53 ± 0.03 eV at room temperature. PzR measurements of GaS were carried out in the energy range between 2 and 5 eV. The low-temperature PzR spectrum obviously shows three doublet-excitonic structures (denoted as series A, B, and C) presented at the energies around 3, 4, and 4.5 eV, respectively. The Rydberg constant and threshold energy of the excitonic series A, B, and C were determined. Transition origins of the A, B, and C series were examined. Temperature dependences of the interband transitions of the gallium sulfide are analyzed. The parameters that describe temperature variations of the transition energies of GaS are evaluated and discussed. © *2006 American Institute of Physics*. [DOI: 10.1063/1.2358192]

I. INTRODUCTION

Layered gallium chalcogenides have very interesting physical properties that have attracted many researchers engaged in this topic for years.[1] GaS is a diamagnetic semiconductor which possesses a crystal lattice with hexagonal structure (space group D_{6h}^4 for β-type GaS).[2] The stacking type of GaS comprises with each monolayer consisting two gallium and two chalcogen closed-packed sublayers in the stacking sequence of S–Ga–Ga–S along the c axis.[3–5] The stacking formula of the $GaSe_{1-x}S_x$ $(0 \leqslant x \leqslant 1)$ mixed compounds with different sulfur stoichiometries may present in three different types of modifications β, ε, and γ phases.[6–8] Generally GaSe layer compound is crystallized in the ε-γ modification. The GaS layer solid belongs to the β stacking phase. The intermediate compounds of $GaSe_{1-x}S_x$ $(0<x<1)$ series with lower and higher sulfur compositions may be presented in dissimilar crystal phase depending on different composition tendency toward to GaSe or GaS.[9–12]

GaX (X=S,Se) were proposed to possess the potential abilities for fabrication of optoelectronic devices applied in red and blue visible regions.[10,13–15] To view their application in the fabrication of photoelectronic devices in visible range, various experimental results regarding the layered GaSe and GaS on luminescence, reflectance, and absorption measurements were proposed.[16–20] GaSe is a well-known material, which possesses a direct gap of about 2.0 eV at room temperature.[21] Gallium sulfide is a wide band-gap semiconductor, which is also a promising material for fabricating the near-blue-light emitting devices.[17] The GaS nanotubes have recently been synthesized and suggested to apply in nanoscale devices.[22] Deposition of gallium sulfide thin film on the GaAs substrate can enhance photoluminescence yield of GaAs by two orders of magnitude.[23] The GaS/GaAs heterostructure can be used as the gate material in a GaAs metal-insulator-semiconductor field effect transistor.[23] A few research works on studying the fundamental gap of GaS were done.[9,17,24,25] One published result claimed that GaS possesses an indirect gap at about 2.59 eV and a direct band gap at approximately 0.45 eV higher in energy.[9] Although some research works regarding the band-gap characteristic of GaS were reported, however, to date, most fundamental studies on the gallium chalcogenides are still focused on GaSe (Refs. 16, 18–20, and 26–28) and the intermediate compounds of $GaSe_{1-x}S_x$ (Refs. 8, 11, and 18) but still very fewer on the GaS compound.

In this paper we report the temperature-dependent optical properties of the interband transitions in gallium sulfide layered solid by using optical-absorption and piezoreflectance (PzR) measurements in the temperature range between 15 and 300 K. The measurements were done in the energy range between 2 and 5 eV. From the comparison of the absorption and PzR spectra at low temperatures, the gallium sulfide layered solid was confirmed to be an indirect semiconductor in which the optical phonons' emission and absorption assist the electronic transition across the gap. Low-temperature PzR spectra of GaS obviously showed three excitonic series (denoted as series A, B, and C) located at the energies near 3, 4, and 4.5 eV, respectively. The transition energies and Rydberg constants for the excitonic series A, B, and C were evaluated. The temperature dependences of the interband transitions for gallium sulfide layered solid are analyzed. The parameters that describe temperature variations of the transition energies of GaS are evaluated and discussed. Based on the experimental results of PzR and absorption measurements together with the temperature dependences of the interband transitions, the origins of the interband transitions are assigned and the probable experimental band picture near the fundamental edge of GaS is realized.

[a]FAX: +886-3-8634200; electronic mail: chho@mail.ndhu.edu.tw

II. EXPERIMENT

Single crystal of GaS solid solution was grown by the chemical-vapor transport method.[29] The method consisted of two steps: First, prior to the crystal growth the powdered compounds of the crystal were prepared from the elements (Ga: 99.999% and S: 99.999%) by reaction at 900 °C for ten days in evacuated quartz ampoules. To improve the stoichiometry, sulfur with 2 mol % in excess was added with respect to the stoichiometric mixture of the constituent elements. About 10 g of the elements introduced into a quartz ampoule [19 mm outside diameter (o.d.), 14 mm inside diameter (i.d.), 15 cm length), which was then evacuated to a pressure of about 10^{-6} Torr and sealed. The mixture was slowly heated to 900 °C. This slow heating is necessary to avoid any explosions due to the strongly exothermic reaction between the elements. For the crystal growth, the chemical transport was achieved by an appropriate amount of material and transport agent (Br_2 about 10 mg/cm^3) placed in a quartz tube (22 mm o.d., 17 mm i.d., 20 cm length), which was cooled with liquid nitrogen, evacuated to 10^{-6} Torr, and sealed. The growth temperature was set as 950 °C $\rightarrow$850 °C with a gradient of −5 °C/cm. The reaction was kept for 350 h to produce large single crystals. The crystals were transparent yellow colored that had the shape of thin layer plates with thickness of 10–100 μm and surface area up to 500 mm^2. Electron probe microanalysis studies showed a slight chalcogen deficiency in the crystals. X-ray diffraction measurements confirmed the β-stacking phase of the hexagonal layers (space group D_{6h}^4). The lattice parameters of the crystal were determined to be $a=3.581\pm0.010$ Å and $c=15.450\pm0.020$ Å, respectively.

For optical-absorption study, measurements of reflectance and transmittance were implemented at near-normal incidence. Transmission intensity was closely monitored to obtain an incidence as close to 90° as possible. The reflectivity studies were done on the as-grown surface (001) and compared against an evaporated gold mirror. Thicker samples with a thickness of about 60–100 μm were utilized for the optical-absorption measurements. Prior to the PzR experiments, the thin specimen of the yellow transparent sheet was precoated with black paint on the rear surface in order to avoid the optical interference in piezomodulation measurements. The PzR measurement was done on the as-grown (001) surface by gluing the back-black-coated thin specimen on a 0.15 cm thick lead-zirconate-titanate piezoelectric transducer driven by a 200 V_{rms} sinusoidal wave at 200 Hz. The alternating expansion and contraction of the transducer subject the sample to an alternating strain with a typical rms $\Delta l/l$ value of $\sim10^{-5}$. A 150 W xenon arc lamp filtered by a 0.2 m monochromator provided the monochromatic light. The reflected light was detected by a photomultiple-tube (PMT) detector and a dual phase lock-in amplifier recorded the signals. The absorption and PzR measurements were done in the temperature range between 15 and 300 K with a temperature stability of about 0.5 K or better. A closed-cycle cryogenic refrigerator equipped a digital thermometer controller was utilized to facilitate the temperature-dependent measurements.

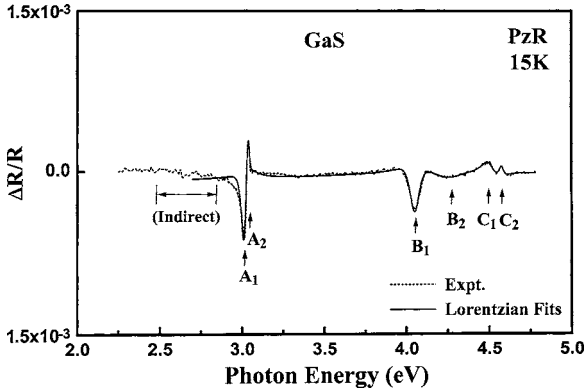

FIG. 1. Low-temperature PzR spectrum of GaS at 15 K. The interband transition energies of the excitonic series A, B, and C are analyzed and indicated by arrows.

III. RESULTS AND DISCUSSION

Displayed in Fig. 1 is the experimental PzR spectrum of GaS at 15 K. The measurements were done in the energy range between 2.25 and 4.75 eV. There are three excitonic series denoted as A, B, and C that can be clearly detected in the PzR spectrum of GaS. The energy locations of A, B, and C are around 3, 4, and 4.5 eV, respectively. There are two excitonic levels ($n=1$ and $n=2$) that can be detected in each excitonic series of A, B, and C. The excitonic features of the experimental PzR spectrum in Fig. 1 can be fitted to a derivative Lorentzian line shape function appropriate for excitonic transitions expressed as[30,31]

$$\frac{\Delta R}{R} = \mathrm{Re}\left[\sum_{n=1}^{2} M_n^{\mathrm{ex}} e^{j\phi_n^{\mathrm{ex}}} (E - E_n^{\mathrm{ex}} + j\Gamma_n^{\mathrm{ex}})^{-2}\right], \tag{1}$$

where $n=1$ or 2, M_n^{ex} and ϕ_n^{ex} are the amplitude and phase of the line shape, and E_n^{ex} and Γ_n^{ex} are the energy and broadening parameter of the interband excitonic transitions. The transition energies for the excitonic series A, B, and C can be, respectively, obtained by fitting the PzR spectrum to Eq. (1). The results are depicted as solid curves in Fig. 1. The obtained transition energies (indicated with arrows) are $A_1=3.020\pm0.002$ and $A_2=3.041\pm0.002$ eV for series A, $B_1=4.051\pm0.005$ and $B_2=4.280\pm0.008$ eV for series B, and $C_1=4.502\pm0.002$ and $C_2=4.578\pm0.002$ eV for series C, respectively. The transition energies of the excitonic sequences A, B, and C can be further analyzed by using the Rydberg series

$$E_j^n = E_j^{n=\infty} - \frac{R_{\mathrm{yd}}^j}{n^2}, \tag{2}$$

where R_{yd}^j is the effective Rydberg constant, $E_j^{n=\infty}$ is the threshold energy of the exciton series, n is the principal quantum number for the transition, and subscript j=A, B, or C refers to the excitonic sequence A, B, or C. As the general trend, the oscillation strength of the $n=1$ exciton level (A_1, B_1, and C_1) is higher than that of the corresponding $n=2$ level (A_2, B_2, and C_2) in Fig. 1. The effective Rydberg constants and threshold energies for series A, B, and C can be obtained by fitting the energy values of the excitonic states to Eq. (2). The obtained values of the threshold energies are

$E_A^{n=\infty}=3.048\pm0.002$ eV, $E_B^{n=\infty}=4.356\pm0.008$ eV, and $E_C^{n=\infty}=4.603\pm0.005$ eV at 15 K and the effective Rydberg's constants are $R_{yd}^{A}=28\pm3$ meV, $R_{yd}^{B}=305\pm10$ meV, and $R_{yd}^{C}=101\pm5$ meV, respectively. From the value of the threshold energy in A exciton series, the direct gap of GaS layered compound is determined to be 3.048 ± 0.002 eV at 15 K. From the information of previous band-structure calculations of β-GaSe,[2,8] we can infer that the excitonic series A is mostly probable originated from the transitions of largely Ga–S bonds at Γ point while series B might come from the bonds of larger Ga–Ga mixed with a little Ga–S in β-GaS. Series C comes from the larger S–S mixed with little Ga–S states.

Temperature dependence of the indirect gap of GaS can be studied by measuring the temperature-dependent absorption spectra from low to room temperature. Absorption coefficient α for the layered material can be determined from the transmittance T_r by taking into account the spectral dependence of the reflectance R using the relation[32]

$$T_r=\frac{(1-R)^2e^{-\alpha d}}{1-R^2e^{-2\alpha d}}, \tag{3}$$

where d is the sample thickness. Equation (3) assumes that there are multiple reflections within the sample, but that they add incoherently due to sample inhomogeneity or a sufficiently large spread of the incident angles. Because αd is large for the sample crystals, the second term in the denominator of the T_r relation can be neglected. The absorption coefficients versus photon energy at various temperatures can be obtained by analyzing the transmittance and reflectance spectral data of GaS using Eq. (3). Analyses of the absorption curves indicate that the absorption coefficient α is proportional to $(h\nu-E_g)^n$ with $n=2.0\pm0.1$. This suggests an indirect allowed transition. The absorption curves of GaS can be further analyzed by taking into account both absorption and emission phonons to determine the band-gap energies (E_g) and the average phonon energies (E_p) for GaS. The absorption coefficient α for a single phonon process of indirect allowed transition can be expressed as[32]

$$\alpha(h\nu)=A_m\left[\frac{(h\nu-E_g+E_P)^2}{\exp(E_P/kT)-1}+\frac{(h\nu-E_g-E_P)^2}{1-\exp(-E_P/kT)}\right], \tag{4}$$

where $h\nu$ is the energy of the incident photon, E_g the band gap, E_p the energy of the phonon assisting the transition, and A_m is related to the matrix elements which is assumed to be a constant. The first term on the right hand side of Eq. (4) corresponds to an absorption of a photon and a phonon, whereas the second term corresponds to an absorption of a photon and emission of a phonon and contributes only when $h\nu\geqslant E_g+E_p$. There are residual absorptions at photon energies below the absorption edge of GaS, which most probably indicates the existence of impurities or defects in the material. In our present study, we have not considered in detail the effect of these impurity or defect states. For simplicity, the residual absorption is assumed to be a constant and subtracted out for the evaluation of the band gap E_g and phonon energy E_p. The data of the compound at different temperatures were then fitted to Eq. (4). Representative results of

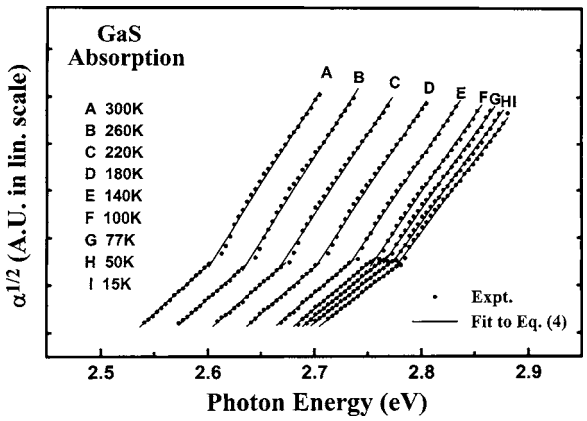

FIG. 2. $\alpha^{1/2}$ vs $h\nu$ of GaS single crystal. The solid circles are representative experimental points deduced from the absorption spectra and the solid lines are the least-squares fits to Eq. (4).

$\alpha^{1/2}$ vs $h\nu$ for GaS are shown in Fig. 2; the solid circles are the representative experimental points deduced from absorption spectra and the solid lines are fitted to Eq. (4). The results strongly indicate that GaS, an indirect band-gap semiconductor and a single phonon, makes important contribution in assisting the indirect transitions. The nonuniform thicknesses and unsmooth sample surface will tend to deviate the incident angles from the normal direction, resulting in some variations in the absorption spectra. Differing values of E_g and E_p could be obtained by fitting a different energy range, thus an error of the order ±0.03 eV and ±7 meV can be deduced for the estimation of E_g and E_p, respectively. According to the fitting analysis of the $\alpha^{1/2}$ absorption curves in Fig. 2, the phonon energy E_p at various temperatures seems to be nearly invariant; it can be estimated to a value of about 26±7 meV. Listed in Table I are the energy values of E_g and E_p of GaS at 300 K together with the indirect gaps and average phonon energies for ReS_2 and $ReSe_2$ (Ref. 33) are included for comparison. The indirect gap of GaS is 2.53±0.03 eV at 300 K. It is in reasonable agreement with the result from the absorption measurement of gallium sulfide by Brebner.[25] The phonon energy of layered gallium sulfide also agrees well with those of the indirect ReS_2 and $ReSe_2$ layer compounds.

Temperature-dependent PzR spectra of the excitonic transitions A_1 and A_2 for GaS are demonstrated in Fig. 3. The dashed lines are the experimental data and the solid lines are least-squares fits to Eq. (1) that yield transition energies which are indicated with arrows. Both the excitonic states A_1 and A_2 simultaneously demonstrate an energy redshift behav-

TABLE I. Values of indirect gap (E_g^{ind}) and average phonon energy (E_p) of GaS at 300 K The energy values of other indirect layer semiconductors of ReS_2 and $ReSe_2$ (see Ref. 33) are also listed for comparison.

Materials	E_g^{ind} (eV)	E_p (meV)	Temperature (K)
GaS[a]	2.53±0.03	26±7	300
ReS_2[b]	1.37±0.02	25±5	300
$ReSe_2$[b]	1.19±0.02	25±5	300

[a]Present work.
[b]Reference 33.

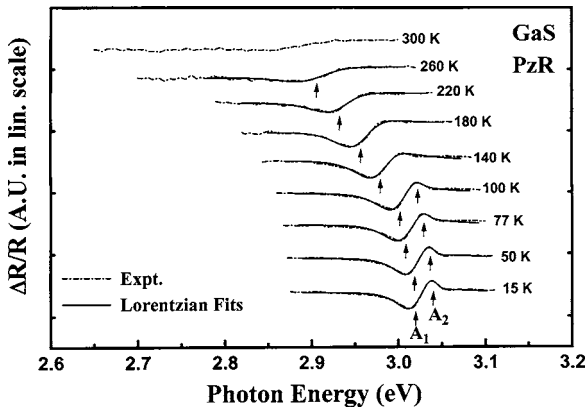

FIG. 3. Temperature-dependent PzR spectra of A exciton series in the temperature range of 15–300 K. The dashed lines are the experimental curves and the solid lines are least-squares fits to Eq. (1) that yields transition energies for A_1 and A_2 which are indicated with arrows.

ior as well as a line shape broadened character with respect to the increase of temperatures. When the temperature rises to 140 K, the thermal ionization effect renders the full dissolve of A_2 state. At a still higher temperature of 300 K, the thermal ionization of A_1 results in a quite flat spectrum in the PzR measurement. The excitonic binding energy of A_1 corresponds to the effective Rydberg constant R_{yd}^{A} (28±3 meV) for A exciton series. The exciton binding energies of A_1 and A_2 are just in good agreement with the temperature values for full ionization of A series (see Fig. 3) by taking them into the thermoenergy relationship of $E_{TH} \cong kT$. Excitonic series A can be regarded as the interband transitions from the largely Ga–S bond at Γ point.

Temperature-dependent PzR spectra of the excitonic transitions of B and C for GaS are demonstrated in Fig. 4. The dashed lines represent the experimental data and the solid lines are least-squares fits to Eq. (1) that yield transition energies for B_1, B_2, C_1, and C_2 which are indicated with arrows. All excitonic features show the energy redshift behavior and linewidth broadened character with respect to the increase of temperatures. The binding energy of B_1 is ~305 meV (i.e., R_{yd}^{B}) that implies that the whole excitonic series of B_1 and B_2 in Fig. 4 could not be dissolved by

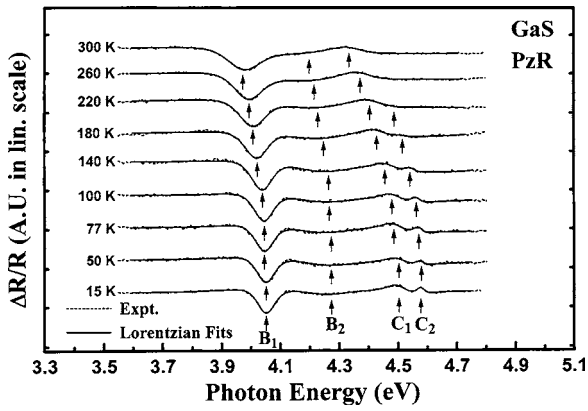

FIG. 4. Temperature-dependent PzR spectra of B and C exciton series in the temperature range of 15–300 K. The dashed lines are the experimental curves and the solid lines are least-squares fits to Eq. (1) that yields transition energies for B_1, B_2, C_1, and C_2 which are indicated with arrows.

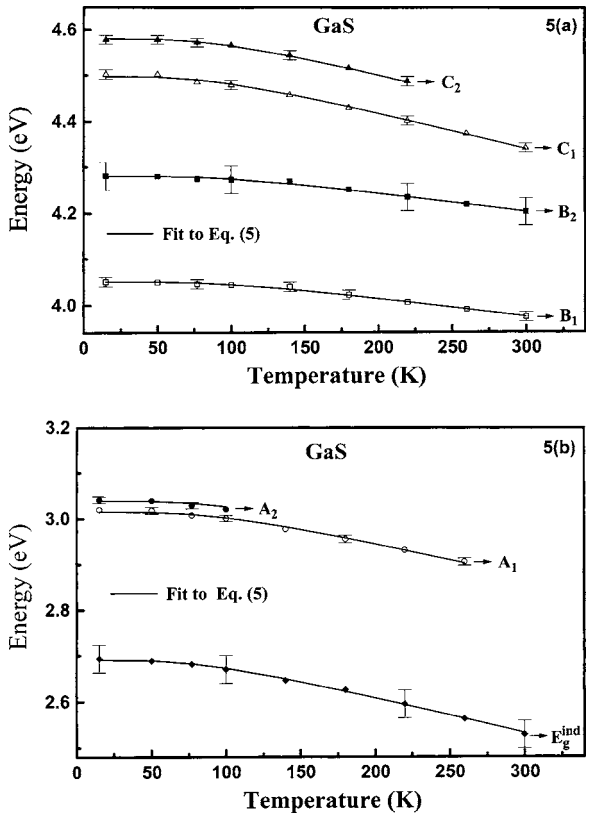

FIG. 5. Temperature dependences of the interband transitions of (a) C_1, C_2, B_1, and B_2, and (b) A_1, A_2, and E_g^{ind} for GaS. The solid curves are least-squares fits to Eq. (5).

thermal ionization even when temperature is up to 300 K. The spectral line shapes of B_1 and B_2 features are rather broad in comparison with those of the A and C excitonic series at 15 K (see Fig. 1). The result implies that the transition origin of B excitons may probably come from the M_1-type critical point (c.p.) in which the saddlelike joint density of states allow more electronic transitions across the gap to widen the spectral line shape. B exciton series can be regarded as the interband transitions originated from largely Ga–Ga mixed with a little Ga–S bonds, which is occurred at M_1 c.p. along T point in β-GaS band.[8] For the exciton series C, the effective Rydberg constant R_{yd}^{C} is about 100 meV that also implied that the binding energy of the C_2 level ($n=2$) is about 25 meV. From Fig. 4, the ionization temperature of C_2 exciton is near 300 K which is in good agreement with the value of the binding energy. The transition origin of the exciton series C is quite different from that of the exciton series B; it can be regarded as the interband excitonic transitions from larger S–S mixed with little Ga–S bonds.

Plotted in Figs. 5(a) and 5(b) are the temperature dependences of the interband transitions of GaS in the temperature range between 15 and 300 K with representative error bars. The solid diamonds represent the indirect gaps of GaS. The hollow (solid) circles, hollow (solid) squares, and hollow (solid) triangles are the energies of A_1 (A_2), B_1 (B_2), and C_1 (C_2), respectively. Temperature dependence of the interband transitions for GaS can be analyzed by a Bose-Einstein-type empirical expression that was proposed by O'Donnel and Chen,[34]

TABLE II. Values of fitting parameters of an expression proposed by O'Donnel and Chen (see Ref. 34) which describe the temperature dependences of the interband transition energies for GaS. The values of fitting parameters for the temperature dependence of the interband transitions of layered ReS_2 (see Refs. 33 and 35) are included for comparison.

Material	Feature	$E_i^{oc}(0)$ (eV)	S	$\langle\hbar\Omega\rangle$ (meV)
GaS	E_g^{inda}	2.690±0.002	4.8±0.4	22±3
	A_1[a]	3.015±0.001	4.7±0.4	26±2
	A_2[a]	3.039±0.001	4.7±0.4	26±2
	B_1[a]	4.051±0.001	2.6±0.3	27±2
	B_2[a]	4.280±0.001	2.6±0.3	27±2
	C_1[a]	4.500±0.002	5.0±0.4	24±2
	C_2[a]	4.580±0.002	5.0±0.4	24±2
ReS_2	E_g^{indb}	1.51±0.02	4.05±0.50	20±2
	E_1^{exc}	1.554±0.005	2.0±0.1	19±3
	E_2^{exc}	1.588±0.005	2.0±0.1	20±3

[a]Present work.
[b]Reference 33.
[c]Reference 35.

$$E_i^{oc}(T) = E_i^{oc}(0) - S\langle\hbar\Omega\rangle[\coth(\langle\hbar\Omega\rangle/kT) - 1], \quad (5)$$

where $E_i^{oc}(0)$ is the transition energy at zero temperature, S is a dimensionless coupling constant related to the strength of electron-phonon interaction, and $\langle\hbar\Omega\rangle$ is an average phonon energy. The excellent fits obtained are shown as solid lines in Fig. 5. The obtained values of $E_i^{oc}(0)$, S, and $\langle\hbar\Omega\rangle$ are listed in Table II. The values of fitting parameters for the temperature dependence of interband transitions of layered ReS_2 (Refs. 33 and 35) are included for comparison. The dimensionless coupling constant S of B_1 and B_2 is lower than the other interband transitions of A_1, A_2, C_1, C_2, and E_g^{ind} due to the temperature-insensitive property of the exciton series B. The values of S for B_1 and B_2 are comparable with those of E_1^{ex} and E_2^{ex} for ReS_2 which come from the metal Re–Re bonds.[35] B series can be regarded as the interband transitions originated from the larger Ga–Ga mixed with little Ga–S bonds. Also seen in Eq. (5), for higher value of kT, $dE_i^{oc}(T)/dT = -2kS$. The calculated value of $dE_i^{oc}(T)/dT$ using the S value in Table II is in good agreement with that obtained from the linear extrapolation slope of the $E_i^{oc}(T)$ data in the high-temperature range of Fig. 5.

Based on the temperature-dependent analyses of the interband transitions for GaS together with the theoretical band-structure calculations of β-GaSe,[2,8] a probable experimental band scheme near the fundamental edge of β-GaS is realized. The conduction band bottom of GaS positioned at M point while the top of valence band at Γ point resulted in an indirect band gap. The indirect-gap transition comes from the mixed states of Ga–S and S–S bonds. Direct transitions of A series are located at Γ point, which come from the interband transitions of largely Ga–S bonding. Excitonic series B comes from M_1 c.p. along T point in which the parallel saddlelike bands allow more electronic transitions to broaden the line shape of the PzR spectra. B excitonic series is originated from the largely Ga–Ga mixed with little Ga–S bonds. Excitonic series C positioned at the highest energy with respect to the series A and B. Exciton series C is originated from the larger S–S mixed with little Ga–S bonds.

IV. SUMMARY

In summary, gallium sulfide layered compound was grown by CVT method using Br_2 as the transport agent. Temperature-dependent optical properties of the interband transitions of GaS were characterized by optical-absorption and PzR measurements in the temperature range between 15 and 300 K. From the comparison of the absorption and PzR spectra at low temperatures the gallium sulfide layered solid was confirmed to be an indirect semiconductor. Low-temperature PzR spectra of GaS obviously showed three excitonic series (denoted as series A, B, and C) located at the energies near 3, 4, and 4.5 eV, respectively. The threshold energies and Rydberg constants for the excitonic series A, B, and C were, respectively, evaluated. The transition origins of the interband transitions are assigned. Excitonic series A is originated from the largely Ga–S bonding at Γ point. Excitonic series B originates from the larger Ga–Ga mixed with little Ga–S bonds along T point at M_1 c.p. Exciton series C comes from the larger S–S mixed with little Ga–S bonds in layered gallium sulfide. Based on the temperature-dependent analyses of the interband transitions together with previous band-structure calculations of β-GaSe, a probable experimental band scheme near the fundamental edge of β-GaS is then recognized.

ACKNOWLEDGMENT

The authors would like to acknowledge the funding support from the National Science Council of the Republic of China under the Grant No. NSC 94-2215-E-259-008.

[1] *Photoelectrochemistry and Photovoltaics of Layered Semiconductors*, edited by A. Aruchamy (Kluwer Academic, Dordrecht, 1992).
[2] M. Schlüter, Nuovo Cimento Soc. Ital. Fis., B **13B**, 313 (1973).
[3] M. Balkanski and R. F. Wallis, *Semiconductor Physics and Applications* (Oxford University Press, New York, 2000), Chap. 1.
[4] F. Levy, *Crystallography and Crystal Chemistry of Materials with Layered Structures* (Reidel, Dordrecht, 1976).
[5] J. F. Sanchez-Royo, D. Errandonea, A. Segura, L. Roa, and A. Chevy, J. Appl. Phys. **83**, 4750 (1998).
[6] A. Kuhn, A. Chevy, and R. Chevalier, Phys. Status Solidi A **31**, 469 (1975).
[7] A. Kuhn, A. Chevy, and R. Chevalier, Phys. Status Solidi A **36**, 181 (1976).
[8] M. Schlüter, J. Camassel, S. Kohn, J. P. Voitchovsky, Y. R. Shen, and M. L. Cohen, Phys. Rev. B **13**, 3534 (1976).
[9] E. Aulich, J. L. Brebner, and E. Mooser, Phys. Status Solidi **31**, 129 (1969).
[10] G. Micocci, A. Serra, and A. Tepore, J. Appl. Phys. **82**, 2365 (1997).
[11] C. C. Wu, C. H. Ho, W. T. Shen, Z. H. Cheng, Y. S. Huang, and K. K. Tiong, Mater. Chem. Phys. **88**, 313 (2004).
[12] C. H. Ho, C. C. Wu, and Z. H. Cheng, J. Cryst. Growth **279**, 321 (2005).
[13] A. Cingolani, A. Minafra, P. Tantalo, and C. Paorici, Phys. Status Solidi A **4**, K83 (1971).
[14] M. Somogyi, Phys. Status Solidi A **7**, 263 (1971).
[15] A. Aydinli, N. M. Gasanly, and K. Göksen, J. Appl. Phys. **88**, 7144 (2000).
[16] A. Balzarotti, M. Grandolfo, F. Somma, and P. Vecchia, Phys. Status Solidi B **44**, 713 (1971).
[17] T. Aono, K. Kase, and A. Kinoshita, J. Appl. Phys. **74**, 2818 (1993).
[18] S. Nüsse, P. Haring Bolivar, and H. Kurz, Phys. Rev. B **56**, 4578 (1997).
[19] S. G. Abdullaeva, V. A. Gadzhiev, and T. G. Kerimova, Phys. Status Solidi B **66**, K119 (1974).

[20]Y. Suzuki and Y. Hamakawa, J. Phys. Chem. Solids **31**, 2217 (1970).
[21]G. Kyazym-zade, R. N. Mekhtieve, and A. A. Akhmedov, Sov. Phys. Semicond. **25**, 840 (1992).
[22]Th. Köhler, Th. Frauenheim, Z. Hajnal, and G. Seifert, Phys. Rev. B **69**, 193403 (2004).
[23]Q. S. Xin, S. Conrad, and X. Y. Zhu, Appl. Phys. Lett. **69**, 1244 (1996).
[24]G. Scamarcio, A. Cingolani, and M. Lugarà, Phys. Rev. B **40**, 1783 (1989).
[25]J. L. Brebner, J. Phys. Chem. Solids **25**, 1427 (1964).
[26]S. Shigetomi, T. Ikari, and H. Nakashima, J. Appl. Phys. **74**, 4125 (1993).
[27]S. Shigetomi, T. Ikari, and H. Nakashima, J. Appl. Phys. **69**, 7936 (1991).
[28]S. Shigetomi, T. Ikari, and H. Nakashima, J. Appl. Phys. **76**, 310 (1994).
[29]C. H. Ho, Y. S. Huang, P. C. Liao, and K. K. Tiong, J. Phys. Chem. Solids **60**, 1797 (1999).
[30]D. E. Aspnes, in *Handbook on Semiconductors*, edited by M. Balkanski (North-Holland, Amsterdam, 1980), p. 109.
[31]F. H. Pollak and H. Shen, Mater. Sci. Eng., R. **10**, 275 (1993).
[32]J. I. Pankove, *Optical Processes in Semiconductors* (Dover, New York, 1975).
[33]C. H. Ho, P. C. Liao, Y. S. Huang, T. R. Yang, and K. K. Tiong, J. Appl. Phys. **81**, 6380 (1997).
[34]K. P. O'Donnel and X. Chen, Appl. Phys. Lett. **58**, 2924 (1991).
[35]Y. S. Huang, C. H. Ho, P. C. Liao, and K. K. Tiong, J. Alloys Compd. **262–263**, 92 (1997).